Beam Transport System of the Kyoto University Cyclotron

AUTHOR(S):

Yanabu, Takuji; Miyake, Kozo; Ikegami, Hidetsugu; Katase, Akira; Yamashita, Sukeaki; Ohama, Taro; Hosono, Kazuhiko; Kakigi, Shigeru; Nguyen, Dai-Ca; Ishiwari, Ryutaro

CITATION:

Yanabu, Takuji ...[et al]. Beam Transport System of the Kyoto University Cyclotron. Bulletin of the Institute for Chemical Research, Kyoto University 1969, 47(2): 123-142

ISSUE DATE:

1969-03-31

URL:

http://hdl.handle.net/2433/76275

Bull. Inst. Chem. Res., Kyoto Univ., Vol. 47, No. 2, 1969

Beam Transport System of the Kyoto University Cyclotron

Takuji YANABU*, Kozo MIYAKE**, Hidetsugu IKEGAMI***
Akira KATASE****, Sukeaki YAMASHITA*****, Taro OHAMA******,
Kazuhiko HOSONO*******, Shigeru KAKIGI********,
Dai-Ca NGUYEN* and Ryutaro ISHIWARI*****

Received March 15, 1969

The beam transport system of the Kyoto University Cyclotron consists of three parts, namely, quadrupole lens magnets, a steering magnet and a beam analyzing magnet. The specifications and beam optical properties of these systems are described.

I. INTRODUCTION

The Kyoto University Cyclotron is a medium size one and can produce 7.5 MeV protons, 15 MeV deuterons and 30 MeV alpha particles. This cyclotron is the second version of a cyclotron proposed and half-constructed before the World War II. In the design study of a new cyclotron in 1952, it was felt quite natural by every staff member in charge, that the extracted beam from the cyclotron should be intense enough to be used in nuclear science experiments. The magnetic field strength of the cyclotron was decided to be 17.5 Kilogauss or higher, based on the fact that the neutron yield from the deuteron bombardment increases more rapidly than the first power of the deuteron energy, and that high field, high energy beam is more useful than the beam obtained with low field, wide dee height cyclotron. The option for a high magnetic field brought some difficulties to the problem of beam extraction and beam focusing. Since the magnetic field gradient is large near and outside of the septum-deflector system, the beam fans out widely in the horizontal direction by the defocusing action of the mag-

* 柳父　琢治，阮　大哥：Laboratory of Nuclear Reaction, Institute for Chemical Research, Kyoto University, Kyoto.
** 三宅　弘三：Institute for Chemical Research, Kyoto University and now at the Department of Physics, Kyoto University, Kyoto..
*** 池上　栄胤：Institute for Chemical Research, Kyoto University and now at the Department of Physics, Tokyo Institute of Technology, Tokyo.
**** 片瀬　彬：Institute for Chemical Research, Kyoto University and now at the Department of Nuclear Engineering, Kyushu University, Fukuoka.
***** 山下　佐明，石割　隆太郎：Institute for Chemical Research, Kyoto University and now at the Department of Physics, Nara Women's University, Nara.
****** 小浜　太郎：Institute for Chemical Research, Kyoto University and now at Central Research Laboratory, Mitsubishi Electric Corporation, Amagasaki.
******* 細野　和彦：Institute for Chemical Research, Kyoto University and now at the Department of Physics, Osaka University, Toyonaka.
******** 柿木　茂：Laboratory of Nuclear Science, Institute for Chemical Research, Kyoto University, Kyoto.

netic field on the way to go through the magnet gap and to the external field. This fan out phenomenon makes the source points of the beam extend over a wide range along the beam course, and then the focusing of the beam becomes troublesome.

The beam profile was obtained graphically by taking into account the real distribution of the magnetic field strength and the static electric field of the septum-deflector system, and the beam spread at the entrance of the focusing magnet was estimated to be about 30 cm in the horizontal direction. To get high intensity beam, it was hoped that the focusing magnet should be as bright as possible. This condition was met with a focusing magnet of short focal length. The beam direction was also determined graphically, and the beam was expected to run through the free space very near the magnet yoke of the cyclotron, therefore the room for beam focusing magnet was not large. From these reasons, quadrupole strong focusing lens magnets were used to focus the extracted beam.

Present situation of the beam transport system of the Kyoto University Cyclotron is shown in Fig. 1. This situation was not achieved at the same time, but was gained step by step. The quadrupole focusing magnets and the beam analyzing magnet were installed in 1956 and the beam steering magnet was constructed in 1964. The broad range magnetic spectrograph, of which the description is given in a later paper, was installed in 1958. Then reasons why these components of the beam transport system were installed separately are mainly due to the lack of funds, but also to the fact that the continuous operation of the cyclotron was not achieved in early stage. Then researches were done using an intermittent beam from the cyclotron and were limitted to the items of nuclear reactions of large cross sections.

In designing the cyclotron, the usefulness of the cyclotron was discussed from several points of view. One purpose was that the cyclotron should be useful as a radioisotope production machine. That is why high magnetic field and high energy as described above were needed to increase the neutron yield. Another purpose was the cyclotron should be useful to nuclear physics research. That is why high intensity beam was needed to research the nuclear phenomena of small cross sections, such as polarization experiment, correlation experiment and so on. One more reason of the need of high intensity beam was to get a beam of small spread in energy. The extracted beam from the cyclotron was estimated to have an energy spread of about 1 %, and the beam intensity would decrease with the decrease of the energy spread.

In those days of the cyclotron designing, 1952~1953, precise nuclear physics measurements were done almost by the Van de Graaf electrostatic accelerators and the energy spread of the beam from these accelerators were about 0.2 %. To compete with the Van de Graaf accelerators in the field of nuclear physics, we hoped to get a beam of 0.1 % energy spread from the cyclotron. The beam analyzing magnet in Fig. 1 was designed so as to achieve this aim. From 1962 on, the continuous operation of the cyclotron became possible and the beam analyzing system began to be utilized in conjunction with the broad range magnetic spectrograph. Continuous operation of the cyclotron brought large

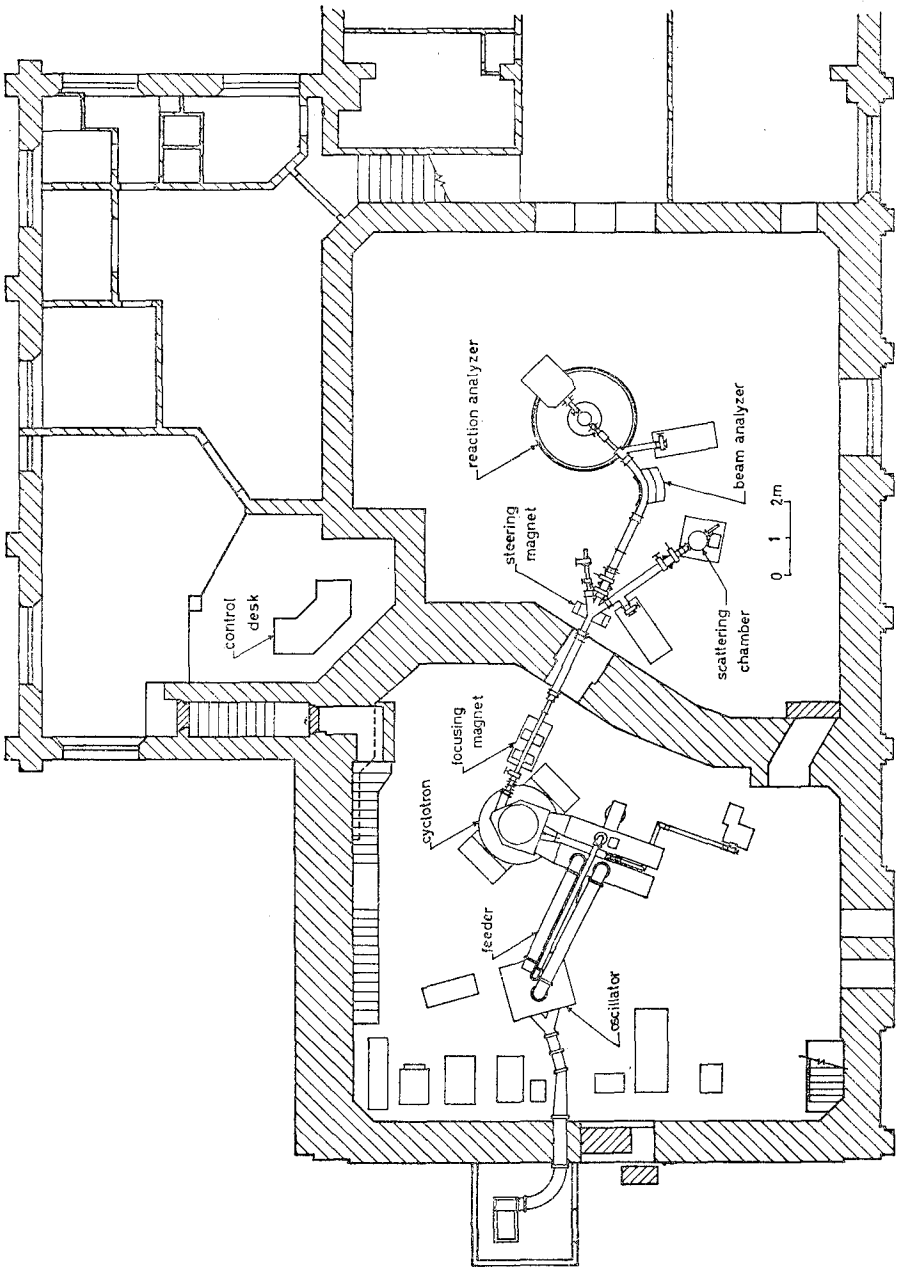

Fig. 1. Lay out of the beam transport system. Figure from K. Kimura : *Bull. Inst. Chem. Res. Kyoto Univ.* 43, 499 (1965).

benefit to the nuclear physics research, and moreover, this operation enabled to use the beam in other field of research. The beam steering magnet was then equipped to serve the multi-purpose usuage of the cyclotron beam.

In the following, the design, construction and performance of the beam transport system are described according to each part of the system.

II. BEAM FOCUSING SYSTEM

II-1. Design

The strong focusing principle was proposed by Courant, Livingston and Snyder[1] in 1952 and today the quadrupole lens magnet is an indispensable part of all the accelerators and beam transport systems. However, in 1955, when the design study of our beam transport system started, examples of quadrupole lens magnets in actual usuage were rather few, and a careful study was needed in order to construct a strong focusing lens magnet without model testing. Our aim was twofold. One was to get as large aperture as possible so to get an intense beam. As described in Section I the extracted beam was estimated to have a spread of 30 cm at the entrance position of the lens magnet. To bring about one third of the beam into focus, the aperture of the lens magnet was decided to be 12 cm. In those days no quadrupole magnet of such a large aperture was experienced. We tried to produce the magnetic field of constant gradient as wide as possible by avoiding the saturation of iron core and by using a pole shape of rectangular hyperbola. Dayton, Shoemaker and Mozlev[2] constructed a 2 inch gap quadrupole magnet with pole tips of circular cross section and obtained constant gradient field within one percent out to 80 % of the radius of the pole gap. Our aim was to get 10 cm or larger range of constant gradient in the gap of 12 cm, so that the pole shape of circular cross section was avoided in spite of the fabrication easiness. The other design principle was to get a focusing system insensible to the position of source point. As stated in Section I the beam profile obtained graphically was of trumpet-shaped. This fact means that the source point of the beam is undetermined and changes according to how much part of the beam is caught by the lens magnet. Therefore, in designing the focusing magnet, it is desirable that the focal point of the beam should be insensible to the position of source point. This condition can be satisfied by the selection of the focusing system of focal length less sensitive to the momenta of the beam particles. A quadrupole magnet is less sensitive to the particle momentum than a sector-type focusing magnet, the reason is as follows.

The focal length of a sector-type deflection magnet is given by

$$f=\frac{a}{\sin\Phi}, \tag{1}$$

where a is the radius of curvature of the particle and Φ is the deflection angle. On the other hand, that of a single quadrupole magnet is given by[1]

$$f=\frac{1}{K^{1/2}\sin K^{1/2}l}, \tag{2}$$

where

$$K=\frac{1}{BR}\frac{dB_y}{dz}=\frac{1}{BR}\frac{dB_z}{dy}, \tag{3}$$

and l is the effective length of this magnet. In Eq. (1) a is proportional to the

particle momentum and therefore the focal length of a sector magnet is proportional to the particle momentum. In Eq. (2), K is inversely proportional to the momentum and therefore the focal length of a quadrupole magnet is a function of the particle momentum lower than first power, that is, the focal length is less sensitive to the particle momentum. Furthermore, the lower sensitivity could be obtained by lessening the field gradient. These were the reasons why we chose the quadrupole magnet as a focusing system and why we were anxious to get large area of constant field gradient.

Figure 2 shows the photo of the quadrupole lens magnet. Figure 3 shows the dimensions of the iron core of a single magnet. The pole profile is of a

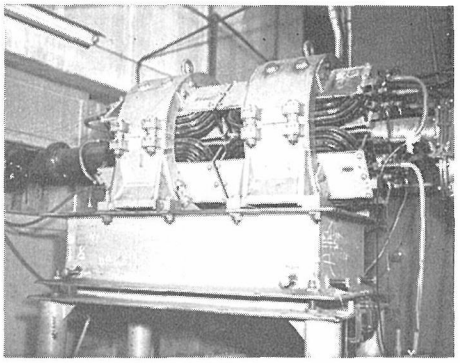

Fig. 2. Photo of the quadrupole lens magnets.

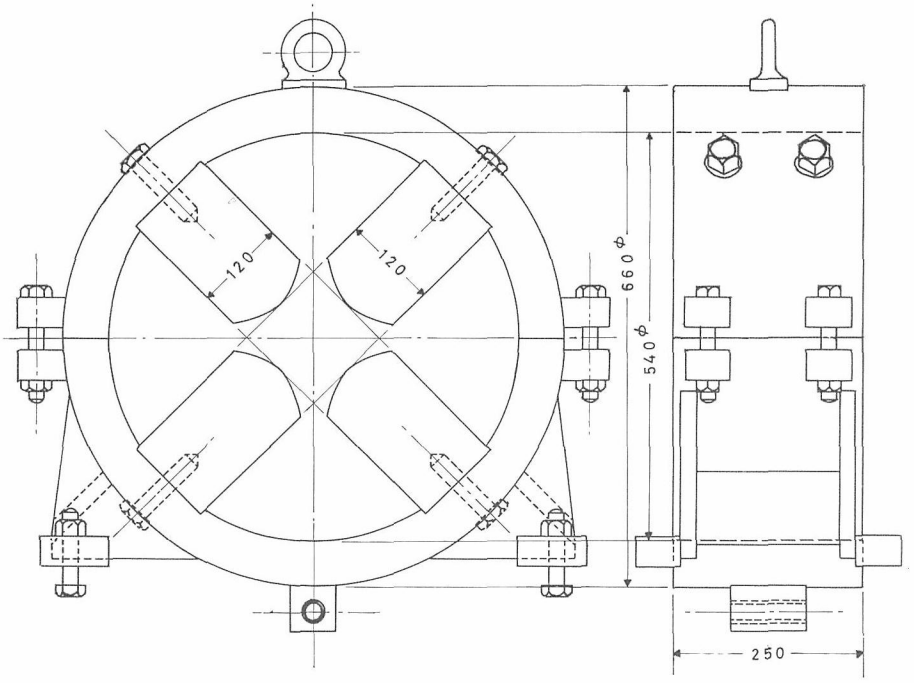

Fig. 3. Dimensions of a quadrupole magnet core (Y-magnet). For Y-magnet, see caption of Fig. 8.

rectangular hyperbola and was made by numerical machining. The error of the machining was less than 0.02 mm.

The coils are excited by a 5 KW motor-generator. The control system of the exciting current is done by regulating an exciting current of the generator. A d. c. amplifier with chopper converter is used to detect error signals.

A pair of magnets are mounted on a common base as shown in Fig. 2. The right side magnet is fixed and the left side magnet can be moved with a screw. The coils of the magnets are excited in parralel and the current to each magnet is adjusted with a rheostat inserted in each circuit.

II-2. Magnetic Field Measurement

The magnetic field distribution was measured according to the method proposed by Elmore and Garrett.[3] Two search coils were set on an arm and this arm was attached vertically to an axis rod which was set along the center line of the quadrupole magnet. Figure 4 shows the photo of this field measuring device. In general, the two-dimensional field distribution is given from the scalar potential[3]

$$V(r,\theta)=\sum_{n=1}^{\infty}\frac{1}{n}h_n r^n \sin n\theta+\sum_{n=1}^{\infty}\frac{1}{n}k_n r^n \cos n\theta\,, \tag{4}$$

where r is the radial distance from the center of the magnet and θ is a polar angle measured from the symmetry axis. In an ideal case of quadrupole magnet, the magnetic field has twofold symmetry and also twofold antisymmetry axes, then for the coefficients h_n in Eq. 4 only those for $n=2$, 6, 10,$\cdots$survive and all k_n's vanish. If $h_n=0$ for $n>6$, the field gradient is given by

$$\frac{\partial H_x}{\partial y}=\frac{\partial H_y}{\partial x}=-h_2\,, \tag{5}$$

and the field gradient is constant everywhere. In reality, the field distribution contains higher order terms of h_n's and also asymmetric part of k_n's. These higher order terms are more effective in the range of large r and break the

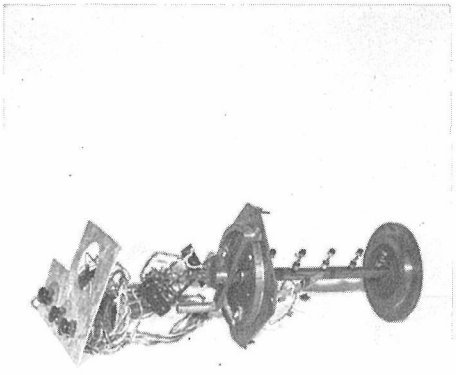

Fig. 4. Photo of the device for magnetic field measurement of a quadrupole magnet.

uniform distribution of field gradient. Then the measure of the goodness of the quadrupole magnet is the ratios h_n and k_n to h_2. The measurement of the field was done at several positions inside the magnet. These positions are indicated in Fig. 5. The search coil angles were changed in 15° steps and 24 fold items of imformations were obtained. The output from coils were fed to a photocell-galvanometer type fluxmeter[4] and the values of coefficients in Eq. 4 were estimated by solving a simultaneous equation.

Figure 5 shows the field gradient as a function of the coil current. 500 Gauss/cm was supposed to be sufficient to focus the beam extracted from the cyclotron from the source point nearest to the quadrupole lens magnet and this value was achieved below the full power of the generator. As seen in Fig. 5, no saturation is observed in the range of exciting current. The exciting current was 21 A. Figure 6 shows the field gradient distributions as functions of the radius. As seen in this figure, the field gradient deviate slightly from h_2 and the deviations become larger at larger radius and at positions nearer the end of the magnet, but at positions 2, 3 and 4, the field gradient is constant within 1 % in the range of radius from center to the full radius of magnet aperture (=6 cm). This good quality is due to the pole profile of the rectangular hyperbola instead of circular shape. Figure 7 shows the field gradient distributions along radius when the excitation are varied. The position of measurement is No. 3 in Fig. 6. At low excitation, the deviation from constant gradient is rather

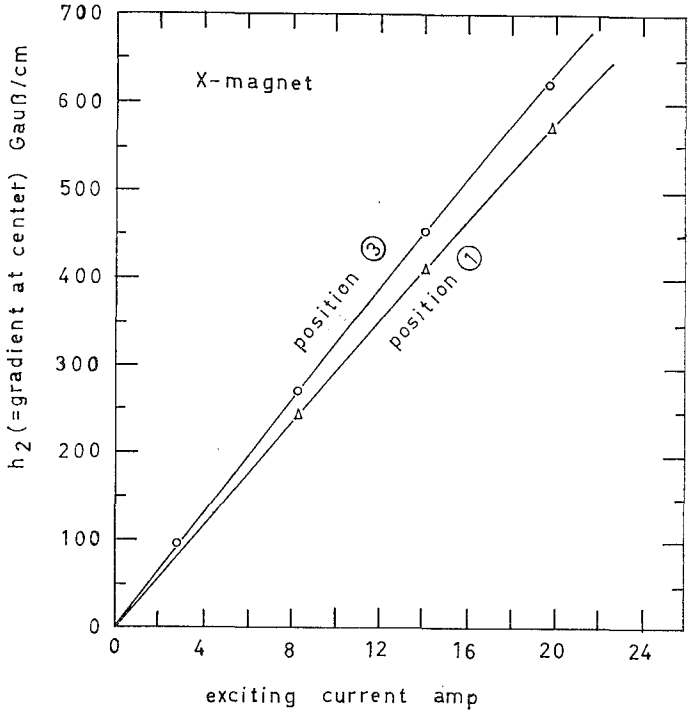

Fig. 5. Excitation curves of a quadrupole magnet (X-magnet). Position 1 or 3 is indicated in Fig. 6. For X-magnet, see caption of Fig. 8.

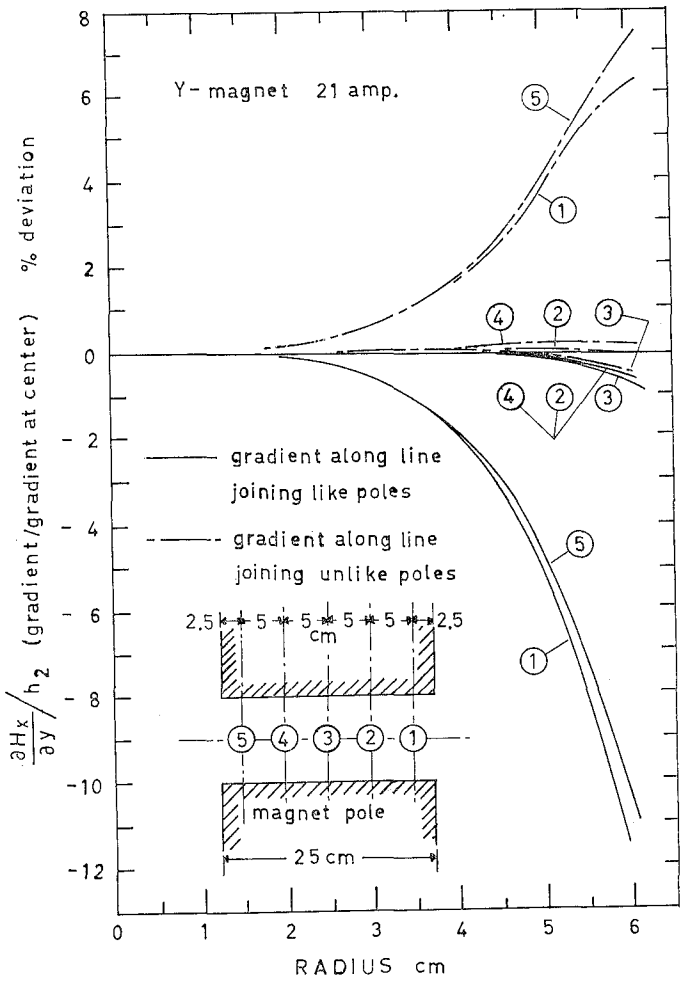

Fig. 6. Deviations of the field gradient from homogeneous distribution. Measured positions are indicated in the figure.

large than in high excitation. This fact is perhaps due to the effect of exciting coils.

II-3. Performance

Beam focusing properties of the lens magnets were tested after the method proposed by Shull *el al.*[5] At the position of source point of the beam analyzing magnet, where in general the slit box is equipped, a quartz plate was set inside the beam duct and the image of the beam was observed. The image varied its shape according to the condition of the field gradient of each quadrupole magnet. Various shapes were rectangle, comet like or spindle like. When the exciting current of one magnet was fixed and that of the other magnet was varied, the image varies its shape from a oblong rectangle to a prolong rectangle in some range of exciting current. An example of the shape variation is shown in Fig. 8. Figure 9 shows the crossing of horizontal and vertical focusing. The shape

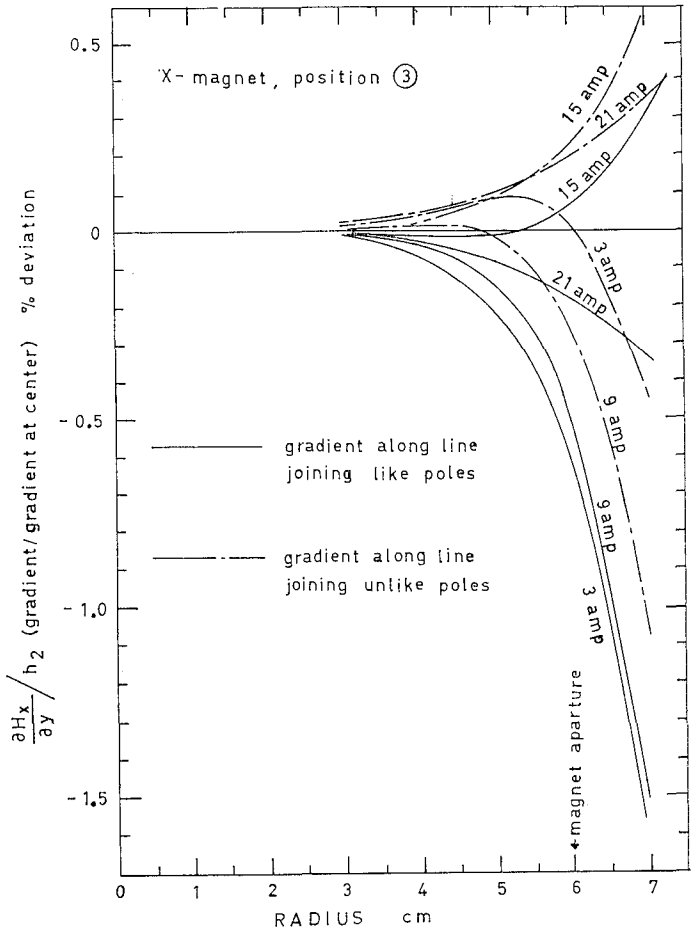

Fig. 7. Field gradient distributions as functions of exciting current and of radius from center.

of the image when double focusing was achieved was a rectangle of about 9 mm wide and 18 mm high.

III. BEAM STEERING SYSTEM

Beam steering is achieved with a steering magnet and the beam is deflected to the right or to the left by 30°. The beam deflected to the right enters into the scattering chamber of 52 cm diameter. Straightforward beam passes through the beam analyzing magnet and enters into the reaction chamber of the broad range magnetic spectrograph. The beam deflected to the left is used to produce radioisotopes. In practice, to neutralize the hysteresis of the magnet, a small demagnetizing current is needed for the straightfoward beam. The power supply of the steering magnet is common with that of the beam analyzing magnet, and the demagnetizing current is given by a power source of small capacity.

The profile of the iron yoke of the steering magnet is given in Fig. 10.

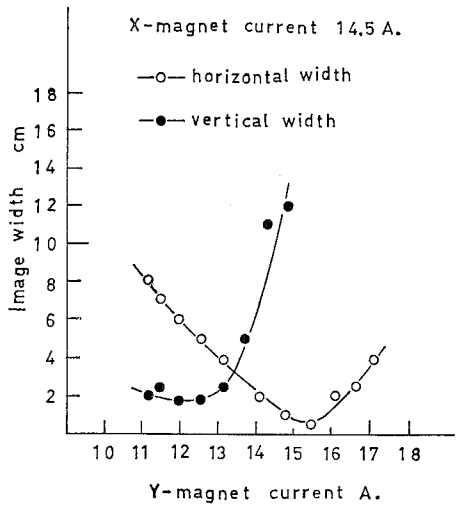

Fig. 8. An example of horizontal and vertical focusing. X-magnet is horizontaly focusing and Y-magnet is vertically focusing. X-magnet is nearer to the cyclotron than Y-magnet.

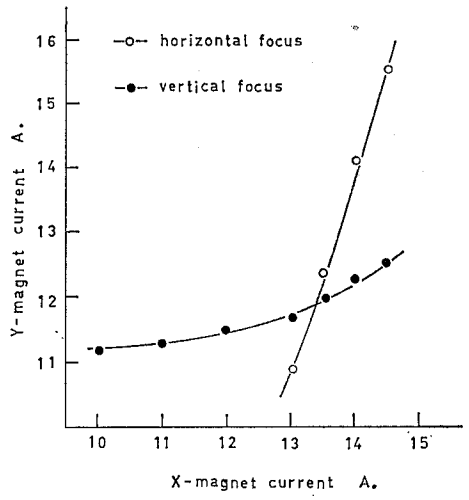

Fig. 9. Double focusing of a proton beam from the cyclotron.

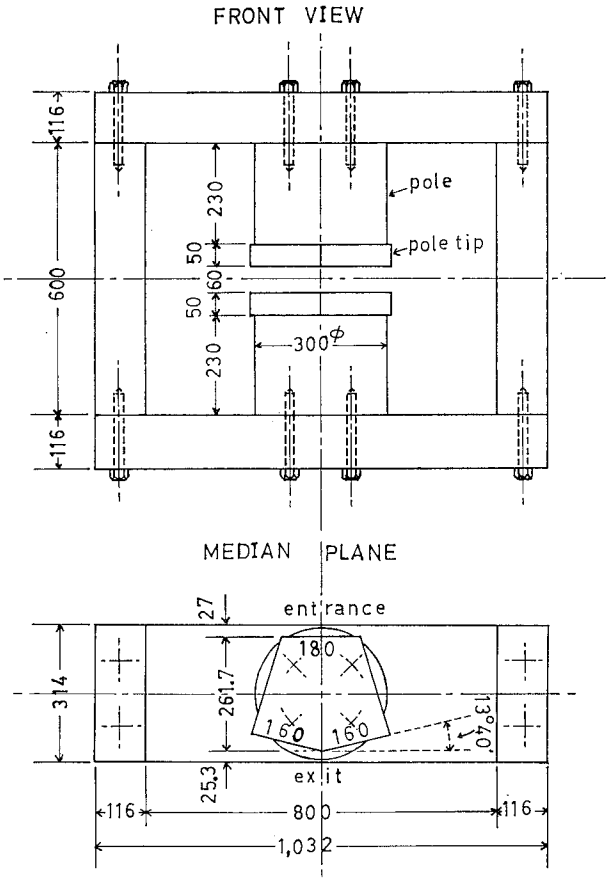

Fig. 10. Dimensions of the steering magnet core.

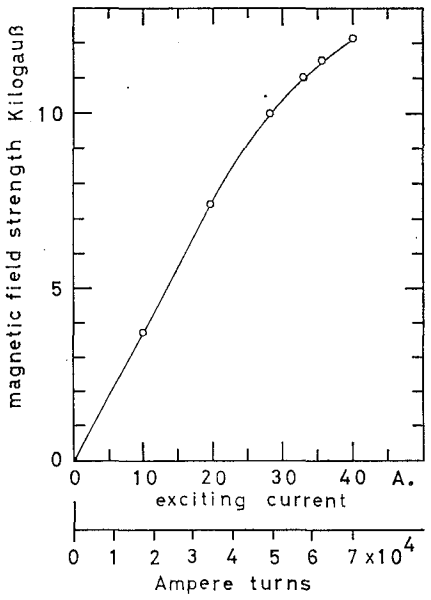

Fig. 11. Excitation curve of the steering magnet.

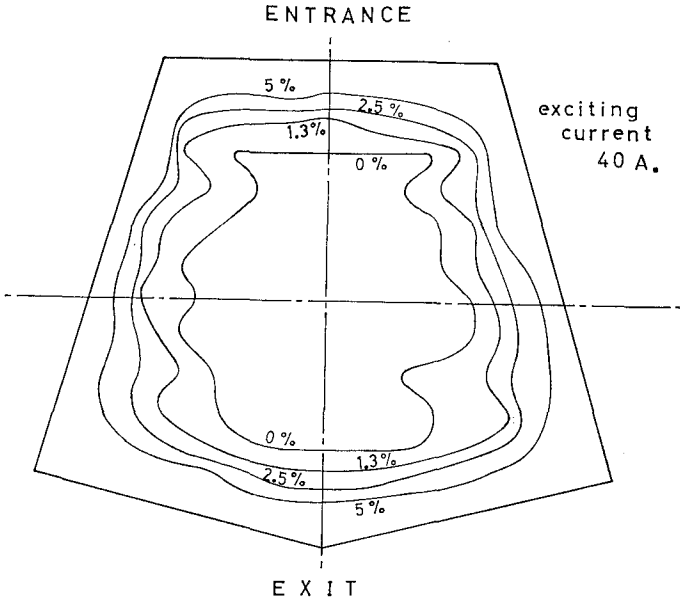

Fig. 12. Field distribution map of the steering magnet. Figures 0 % and so on mean the percentage drop of the field relative to that at center.

Figure 11 gives the excitation curve of the steering magnet. This curve was obtained by measuring the magnetic field at low excitation with a semi-conductor flux meter and at high field (>10 KGauss) with an NMR method. The semi-conductor flux meter was of large error, so that this excitation curve is not so accurate but sufficient to practical use.

Figure 12 shows the field distribution map of the steering magnet at 40 A excitation. As seen from Fig. 11, at 40 A excitation, the magnetic field exceeds the intended value for experimental purpose ($\simeq$10 KGauss), because when the field distribution was measured, accurate value of the field was unknown and it was supposed from the semi-conductor flux meter measurement that the field was near the value of 10 KGauss at 40 A excitation. The field distribution was obtained by measuring the field strength at each mesh point of 2 cm distance and deviations relative to the value at the center position were plotted. In constructing the steering magnet, the yokes of the magnet were made from low carbon steel bullet of sheet iron*, and poles from soft electro-magnetic iron of Japanese Industrial Standard. Poles and pole tips in Fig. 10 were machined from one block material and caution was paid to lessen the unnecessary magnetic resistance. The field deviations would be smaller than that given in Fig. 12 at the field used to deflect the beam by 30°.

In the design study of the steering magnet, the profiles of poles were determined to give no focusing, but from our experience, the exciting current of the quadruple lens magnets should be a little less than those values of no deflection.

IV. BEAM ANALYZING SYSTEM

IV-1. Design

The aim of the beam analyzing system was to get a beam of exactly defined energy within the width of 0.1 %. As described in Section I of this paper, in those days when the cyclotron was constructed, high precision experiment in nuclear physics was done by using the Van de Graaf accelerator and the beam energy spread was about 0.2 %. To get informations about highly excited states of medium and heavy nuclei, more accurate measurement was needed and more precise determination of the beam energy was hoped. In practice, to get a precisely determined beam is a necessary condition of a precision experiment, but is not the sufficient. The intensity of the separated beam, the straggling of the beam through the target material, kinematical variation of the energy of particles emitted from the target, the energy resolution of the particle detecting system, all these experimental conditions should be balanced and satisfy the need of precise experiment. Our aim of the beam analyzing system, 0.1 % energy spread, is a result of the compromise among those conditions.

The design of the beam analyzing system was determined by taking into account the following conditions.

1. To get necessary resolution, the momentum dispersion was made large by taking the radius of curvature as large as one can afford economically.

2. The maximum magnetic rigidity of the analyzing field was determined to be 8×10^5 Gauss-cm, equal to the magnetic rigidity of the beam from the cyclotron, and the magnetic field was hoped to be linear to the exciting current, so that the maximum magnetic field was determined to be 10 K Gauss and the

* We are indebted to Sumitomo Metal Industries Ltd. for the offer of these bullets.

radius of curvature of the particle to be 80 cm.

3. To get double focusing, the oblique entrance method was adopted. The merit of the oblique entrance method is, besides the double focusing effect, one can expect with this method a smaller magnification and a larger momentum spread than with the normal entrance method. These effects are helpful to get better resolution.

4. The focal length of the analyzing magnet is limited from the dimensions of the experimental area. The deflection angle of the analyzing magnet was decided to be 70° so as to set relevantly the beam transport system, the scattering chamber and the particle analyzing magnet in the experimental area.

5. To diminish the second order aberration, the boundary of the magnetic field in the entrance and exit is made curved according to the Hintenberger proposal.[6]

6. To keep the effective boundary of the magnetic field as close to the designed boundary as possible, the fringing flux corrections were done after the proposal of Coggeshall[7] and after the modified formula suitable to the oblique

Table I. Design Parameters of the Beam Analyzing Magnet.

ϕ	c	l'	l_d''	ε_1	ε_2	m	X_G	T_G for $\frac{\Delta p}{p}=0.05\%$	R_1	R_2
70°	80cm	2.4307 (=194.46cm)	2.4308 (=194.46cm)	34°25′	0°	0.7286	1mm	1.177mm	∞	3,462mm

Notations: ϕ, deflection angle. c, radius of curvature of the beam. l', distance from source point to entrance boundary in units of c. l_d'', distance from exit boundary to image point in units of c. ε_1, entrance angle measured from the normal to the boundary. ε_2, exit angle. 0° means the beam goes out normally to the boundary. m, magnification. X_G, source width. T_G, lateral spread at image point. R_1, radius of curvature of entrance boundary. R_2, radius of curvature of exit boundary to obtain second order focusing.

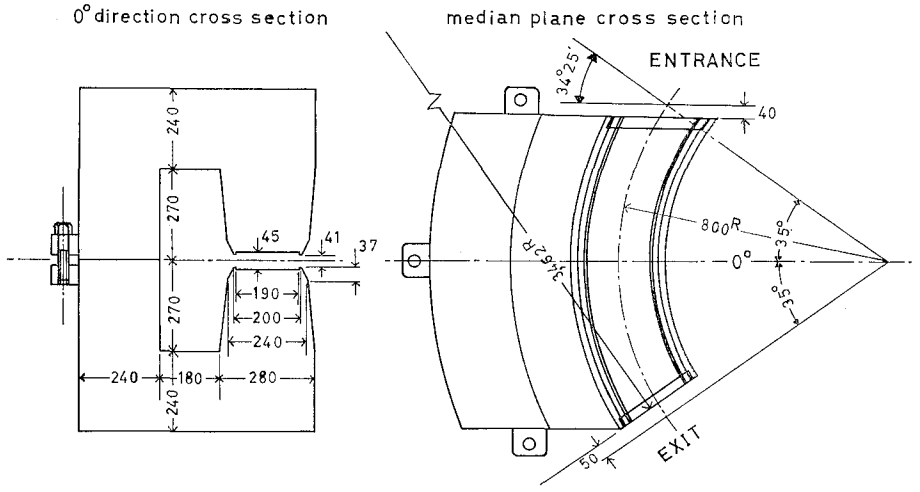

Fig. 13. Dimensions of the beam analyzing magnet core.

entrance method.

The ion-optical parameters of the beam analyzing system are given in Table I and the dimensions and profiles of the magnet core are shown in Fig. 13. As shown in Fig. 13, the fringing flux correction in the entrance were done by designing the real boundary of the magnet withdrawn from the virtual boundary by 40mm. The basic formula for the fringing field correction is given in Appendix. The fringing field correction in the exit of the beam were bone by setting the real boundary withdrawn by 50 mm. This value is 1.2 times the magnet gap, and according to our experience, this correction was somewhat over-estimated. We believe that the fringing field correction is sufficient to withdraw the boundary by one magnetic gap when the magnetic field is used below the saturation of the iron core.

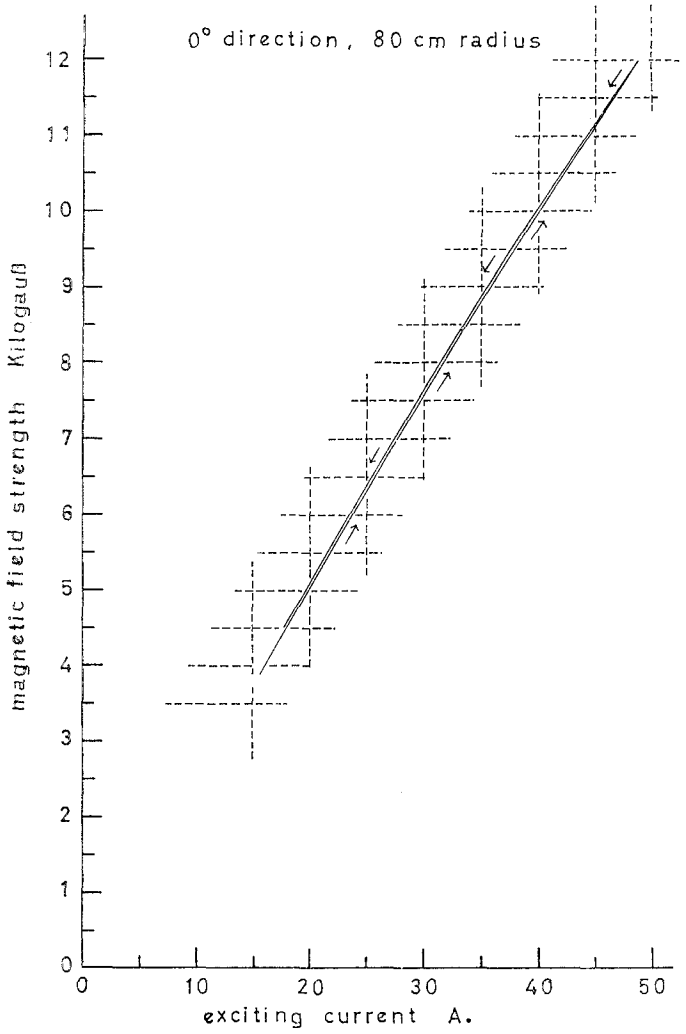

Fig. 14. Excitation and hysteresis curve of the beam analyzing magnet. The field was measured with an NMR method and the data points are omitted for read out convenience.

IV-2. Construction and performance

The beam from the cyclotron is focused by the quadrupole lens magnets and enters into the steering magnet. When deflected to the right by the steering magnet, the beam is focused at the entrance iris of the collimator of the scattering chamber. When there is no deflection, the beam is focused at the slit system about 195 cm apart from the entrance boundary of the beam analyzing magnet. The slit system is composed of the vertical slit and the horizontal slit and forms the source point of the beam analyzing magnet. When the degradation of the beam energy is needed, stacked foils are inserted just in front of the slit system.

The beam then enters into the magnetic field of the beam analyzer, of which the field strength is measured by a proton NMR method at the position about 18 cm inward from the entrance edge of the magnet. The beam duct is made of non-magnetic stainless steel and is mounted between the gap of the magnet poles. Since the analyzing magnet is of C-type, spacers made of brass and finished manually within the error of 0.01 mm are placed outside the stainless duct and just inside the Rose shim of the magnet poles, to prevent the pole gap widths from non-uniform distribution.

Figure 14 shows the excitation curve of the analyzer magnet. The field strength was measured with the NMR method and the probe was set at radius of 80 cm and at 0° direction shown in Fig. 12. Figure 15 gives the radial distribution of the magnetic field along 0° direction in Fig. 13. This distribution was obtained by measuring the field strength at each radius with the NMR method.

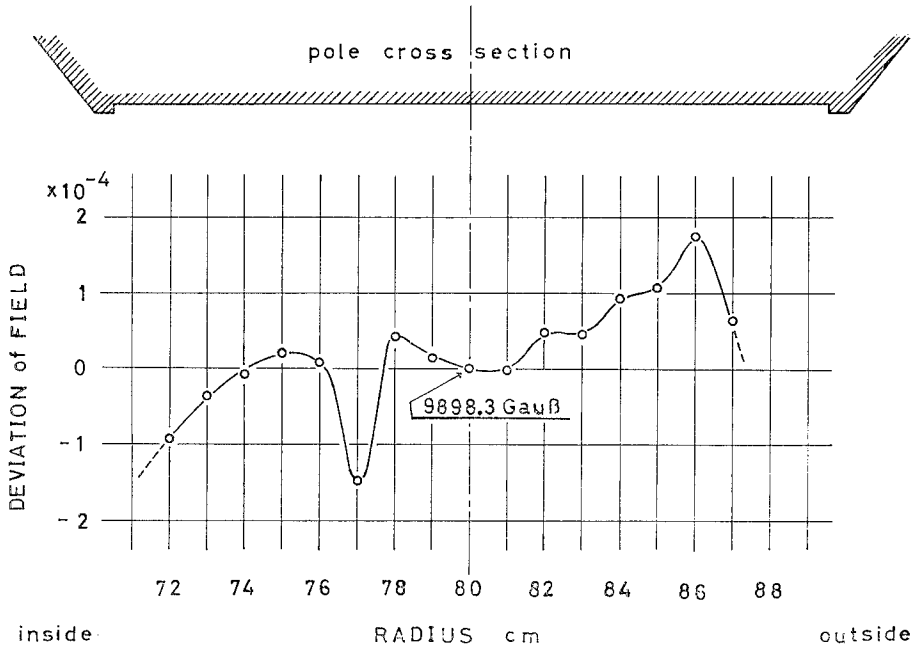

Fig. 15. Radial direction distribution of the analyzing field. Normalized to the value at center.

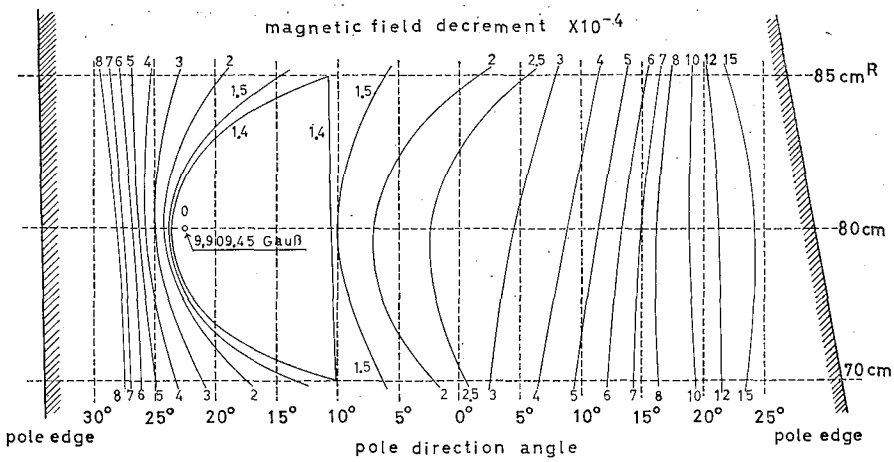

Fig. 16. Field distribution map of the beam analyzing magnet. The dotted lines show the mesh points of observation. Figures 0, 1.4 and so on indicate the drop of field in units of 10^{-4} relative to the highest field (figure 0).

The field is uniform within 0.2 % over the radial range thus measured. Figure 16 gives the field distribution map of the analyzing magnet. An NMR probe was set at each mesh of the direction angle and radius and the field strengh distribution was plotted relative to the maximum field in the observation. Figures in Fig. 16 give the field decrement in units of 10^{-4}.

The effective radius of this analyzing magnet was estimated as follows. Alpha particle source of Po^{212} was placed at the source point of the magnet. The Po^{212} source had a rectangular shape of 2.1 mm width times 4 mm height. The object slit equipped at the source point was adjusted to have 2.1 mm width. The slit system equipped at the entrance of the magnet was set to have 65 mm width. A 500 μm thick solid state detector was placed at the image point of the analyzing magnet and counted the alpha particles as a function of the magnetic field. The magnetic field was measured with an NMR probe inserted to the magnet gap. From known value of magnetic rigidity of ThC′.

$$H\rho(Po^{212}\alpha) = 427060 \pm 20 \text{ Gauss-cm}^{8)},$$

the effective radius of curvature of the magnet was determined to be

$$\text{effective radius} = 78.9012 \pm 0.0055 \text{ cm}.$$

This value is less than the designed value (=80 cm) by about 1 cm. This difference may be due to the over-cutback of the fringing field correction.

The beam analyzing system has been used since 1963 coupled with the broad range magnetic spectrograph. The momentum resolution of the analyzer is not measured directly, but the data obtained with the broad range spectrograph pointed out that the beam energy width is less than 0.1 % when a slit of 1 mm wide is set at the source point and a slit of 0.73 mm is set at the image point. Hosono *el al.*[9] obtained an alpha particle beam of 55 KeV energy spread and measured precisely the energy loss of 28 MeV alpha particles through various

materials. Nguyen[10] had resolved in his deuteron inelastic scattering experiment the 6.06 MeV state of O^{16} from neighbouring 6.14 MeV state succesfully. About the problem to obtain a beam of 0.1 % energy width, the analyzing system has been proved to be reliable.

V. CONCLUSION

Various parts of the beam transport system of the Kyoto University Cyclotron were constructed separately during a long time interval. The memory of the initial stage of construction has faded away and detailed explanations of the accessory devices such as slit systems, evacuation systems and structures of duct systems were omitted for the sake of inaccurate description and for time saving. This paper was written in order to give the forthcoming young students in our laboratory the idea and principle of the beam transport system design. To-day a computor program is available to the design of the beam transport system as a combination of linear optics of charged particles, but from our experience, non-linear effects such as the fringing field distribution make it difficult to construct an ideal system of beam transport problem and if money and time is sufficient, bench test of beam transport system is very useful and indispensable.

ACKNOWLEDGMENTS

The authors would like to thank Prof. K. Kimura and Prof. S. Shimizu for their guidance and encouragements throughout the work. They also acknowledge Dr. J. Kokame, now at the Institute for Nuclear Study, University of Tokyo, for his critical discussions. Finally, the Grant-in-aid of Ministry of Education supported the expenditure of this work and is appreciated.

APPENDIX

Fringing field correction for oblique entrance.

As discussed by Coggeshall,[7] the fringing field correction is determined from the integral distribution of the fringing field.

If we define a function $h(x)$ as

$$H(x)=H_0h(x) \ , \qquad \text{(A-1)}$$

where $H(x)$ is the magnetic field at x and H_0 is the field far inside the pole boundary. The coordinates and the beam trajectory are shown in Fig. A-1.

In the case of normal entrance (course 1 in Fig. A-1), following Coggeshall, the beam trajectory is given by the differential equation:

$$\frac{dy}{dx}=-\frac{f}{(r^2-f^2)^{1/2}} \ , \qquad \text{(A-2)}$$

where

$$f=\int_{-\infty}^{\infty} h(x)dx$$

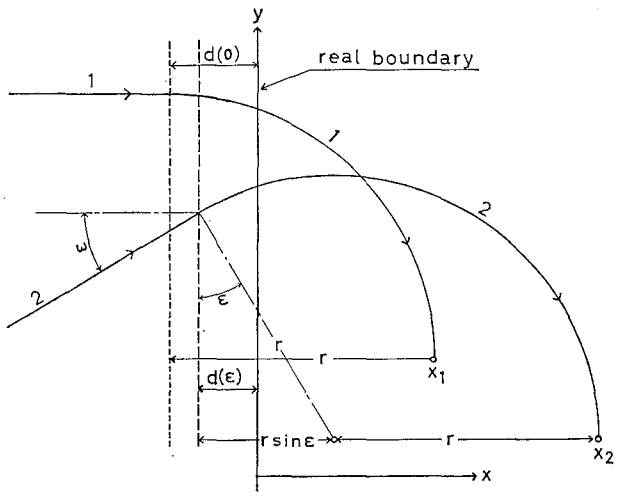

Fig. A-1.

and

$$r=\frac{pc}{H_0 e} \ .$$

In this case,

$$\frac{dy}{dx}=-\infty \text{ at } x=x_1 \ ,$$

then

$$r=f_1=\int_{-\infty}^{x_1} h(x)dx \ , \tag{A-3}$$

and the fringing field distance $d(0)$ is given by

$$d(0)=r-x_1=\int_{-\infty}^{x_1} h(x)dx-x_1 \ . \tag{A-4}$$

In the case of oblique entrance, (course 2 in Eig. A-1), however, the Eq. (A-2) should be modified by setting

$$f=\int_{-\infty}^{x_1} h(x)dx+g \ , \tag{A-5}$$

where g is a constant and determined from the condition

$$\frac{dy}{dx}=\tan\epsilon \quad \text{at } x=-\infty$$

and

$$\tan\epsilon=-\frac{g}{(r^2-g^2)^{1/2}} \ , \tag{A-6}$$

when expressed as

$$g=-kr \ .$$

Eq. (A-6) gives

$$k\simeq\tan\epsilon\left(1-\frac{1}{3+\frac{2}{\tan^2\epsilon}}\right) . \tag{A-7}$$

At $x=x_2$, as seen from Fig. A-1, $\frac{dy}{dx}=-\infty$ and then

$$r^2=f_2^2 \quad \text{at } x=x_2 \ .$$

From the consideration of the sign, this equation leads

$$r=f_2 \ , \tag{A-8}$$

and

$$f_2=\int_{-\infty}^{x_2} h(x)dx+g \ . \tag{A-9}$$

Referring the Eq. (A-3), Eq. (A-8) is rewritten as

$$f_2=\int_{-\infty}^{x_1} h(x)dx+\int_{x_1}^{x_2} h(x)dx+g=r+x_2-x_1+g \ ,$$

because

$$h(x)=1 \quad \text{from } x=x_1 \text{ to } x=x_2 \ .$$

Then we have

$$r+x_2-x_1+g=r$$

from Eq. (A-8). This leads to

$$x_2=x_1-g \ . \tag{A-10}$$

On the other hand, it is seen from Fig. A-1 that

$$r\sin\epsilon+r=d(\epsilon)+x_2 \ .$$

Therefore

$$d(\epsilon)=r+r\sin\epsilon-x_2=r-x_1+r\sin\epsilon+g$$

from Eq. (A-10). Then

$$d(\epsilon)=d(0)+r\sin\epsilon+g=d(0)+r(\sin\epsilon-k) \ . \tag{A-11}$$

The value of the parenthesis is negative, so that $d(\varepsilon)$ is smaller than $d(0)$ when the beam enters into the magnet boundary with positive ε. The cut-back of the entrance boundary of the beam analyzer magnet was determined from Eq. (A-11).

REFERENCES

(1) E. D. Courant, M. S. Livingston and H. S. Snyder, *Phys. Rev.*, 88, 1190 (1952).
(2) I. E. Dayton, F. C. Shoemaker and R. F. Mozlev, *Rev. Sci. Inst.*, **25**, 485 (1954).
(3) W. C. Elmore and M. W. Garrett, *Rev. Sci. Inst.*, **25**, 480 (1954).
(4) R. H. Dicke, *Rev. Sci. Inst.*, **19**, 533 (1948).
(5) F. B. Shull, C. E. MacFarland, and M. M. Bretscher, *Rev. Sci. Inst.*, **25**, 364 (1954).
(6) H. Hintenberger, *Rev. Sci. Inst.*, **22**, 748 (1951).
L. A. König and H. Hintenberger, *Z. Naturforsch.*, **12a**, 377 (1957).
(7) N. D. Coggeshall, *J. Appl. Phys.*, 18, 855 (1947).
(8) A Ritz, *Helv. Phys. Acta*, **34**, 240 (1961).
(9) K. Hosono, R. Ishiwari and Y. Uemura, *Bull. Inst. Chem. Res., Kyoto Univ.*, **43**, 323 (1965).
(10) D. C. Nguyen, *J. Phys. Soc. Japan*, **21**, 2462 (1966).